UCRL-JC-124887
PREPRINT

Status of the National Ignition Facility Project

J. A. Paisner, W. H. Lowdermilk,
J. D. Boyes, M. S. Sorem, and J. M. Soures

This paper was prepared for and presented to
IAEA-TCM 1997 Conference
Osaka, Japan
March 10-14, 1997

April 1, 1997

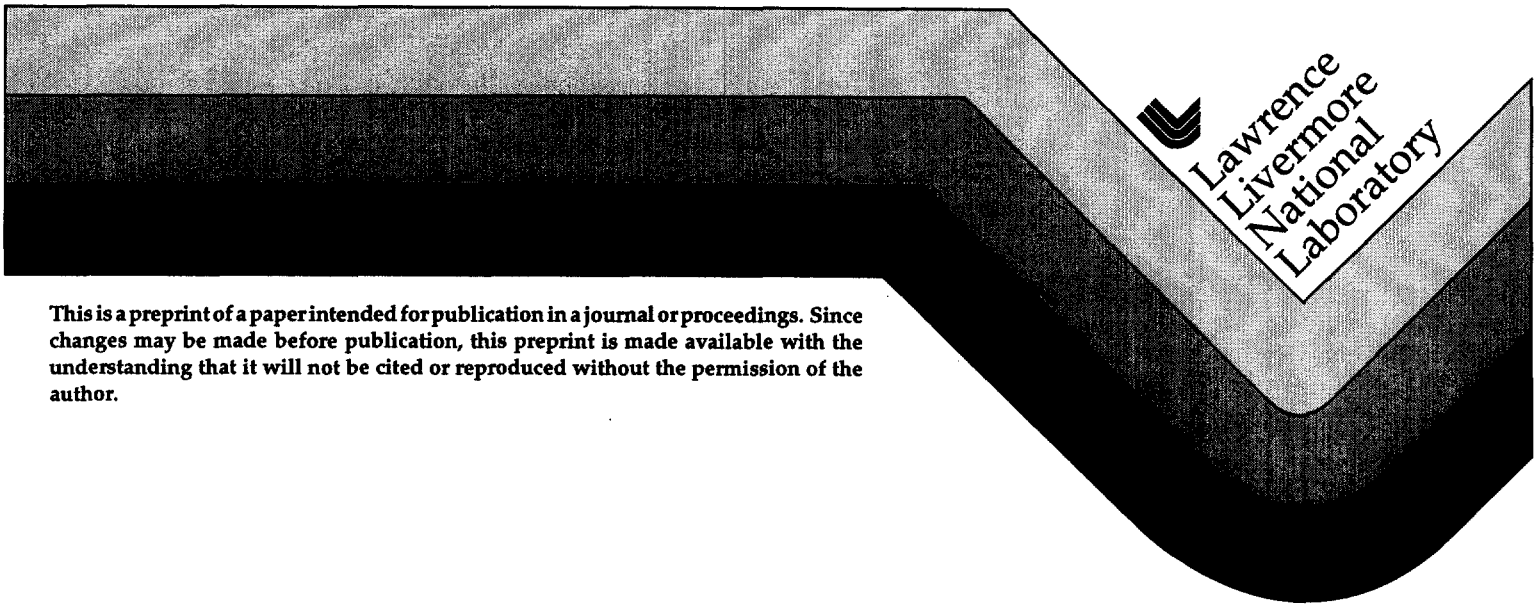

Status of the National Ignition Facility Project

Jeffrey A. Paisner, W. Howard Lowdermilk

Lawrence Livermore National Laboratory

John D. Boyes

Sandia National Laboratory

Allbuquerque New Mexico

Michael S. Sorem

Lol Alamos National Laboratory

Los Alamos New Mexico

John M. Soures

Laboratory for Laser Energetics, University of Rochester

Rochester, New York

ABSTRACT

The ultimate goal of worldwide research in inertial confinement fusion (ICF) is to develop fusion as an inexhaustible, economic, environmentally safe source of electric power. Following nearly thirty years of laboratory and underground fusion experiments, the next step toward this goal is to demonstrate ignition and propagating burn of fusion fuel in the laboratory. The National Ignition Facility (NIF) Project is being constructed at Lawrence Livermore National Laboratory (LLNL), for just this purpose. NIF will use advanced Nd-glass laser technology to deliver 1.8 MJ of 0.35-μm laser light in a shaped pulse, several nanoseconds in duration, achieving a peak power of 500 TW. A national community of U.S. laboratories is participating in this project, now in its final design phase. France and the United Kingdom are collaborating on development of required technology under bilateral agreements with the US. This paper presents the status of the laser design and development of its principal components and optical elements.

1 NATIONAL IGNITION FACILITY

Based on the theoretical and experimental results to date, accurate predictions can be made of target ignition and gain as a function of driver pulse energy. The next step toward inertial confinement fusion (ICF) in the laboratory is to map out

the ignition and gain curves for direct-and indirect-drive ICF. The National Ignition Facility (NIF), now under construction at LLNL, is expected to accomplish this goal.

Experiments to be conducted on the NIF will determine the minimum energy required for ICF capsule ignition, and map out the scaling of target gain as a function of laser energy. With this information, targets optimized for future inertial fusion energy (IFE) power plants can be designed with greater confidence. Requirements established for the NIF are based on calculations, such as those shown in Fig. 1, that represent the margin above ignition as a function of laser energy and power for both indirect drive (Fig. 1a) and direct drive (Fig. 1b). S. W. Haan, S. M. Pollaine, J. D. Lindl, L. J. Suter, R. L. Berger, L. V. Powers, W. E. Alley, P. A. Amendt, J. A. Futterman, W. K. Levedahl, M. D. Rosen, D. P. Rowley, R. A. Sacks, A. I. Shestakov, G. L. Strobel, M. Tabak, S. V. Weber, G. B. Zimmerman, W. J. Krauser, D. C. Wilson, S. V. Coggeshall, D. B. Harris, N. M. Hoffman, and B. H. Wilde [1] The shaded regions in energy-power space corresponding to the achievement of ignition and gain are bounded along the top by the onset of laser plasma instabilities and on the bottom by hydrodynamic instabilities. In both direct and indirect drive, the minimum energy and power required for ignition is approximately 1 MJ and 400-450 TW. However, the driver must have a capability above this minimum ignition energy to account for experimental uncertainties. For this reason, the primary energy and power

requirement for the NIF was established as 1.8 MJ at 500 TW. This and other primary performance requirements for the NIF are summarized in Table 1.

Table 1. Top level performance specifications for NIF

Energy (measured at hohlraum entrance hole)	1.8 MJ
Peak power	500TW
Wavelength	0.35 μm
Pulse shaping	Flexible (dynamic range > 50)
Beam power balance	<8% rms over 2 ns
Beam pointing accuracy	<50 μm
Focal spot diameter	<500 μm at the laser entrance hole
Prepulse	$<10^8$ W/cm^2
Pulse simultaniety	<30 ps
ICF target capability	Cryogenic and non-cryogenic
Annual fusion yield capability	50 shots with yield 20 MJ 1200 MJ/y annual yield

The National Ignition Facility[2], shown in Fig. 2, consists of a multibeam Nd-glass laser, target area and ignition diagnostics housed in the main Laser and Target Area Building, and an Optics Assembly Building. The laser, 50 times more powerful than the Laboratory's Nova laser, has a compact, multipass, multisegment architecture, allowing it to fit into a building only about twice the size of the Nova Building. The Laser and Target Area Building, 200 meters long, 85 meters wide, and 35 meters tall above the target chamber, has a U-shaped floor plan to facilitate later addition of target chambers should their need arise.

The laser has 192 independent laser beams, each with 40 cm square aperture. The optical arrangement of each beam is shown in Fig. 3. For economy and efficiency, beams will be grouped into four large arrays, four beams high and twelve beams wide. The complete laser will contain more than 9000 optical elements with aperture of 40×40 cm^2, or greater, and approximately 30,000 smaller optics. Table 2 summarizes the quantities required of the large optical elements. All components of the main laser beamline are mounted overhead to provide for maximum cleanliness during assembly and maintenance.

Table 2. Large aperture optical components required for NIF

Component	Material	Number Required
Amplifier slabs	Nd-Phosphate glass	3456
Lenses	Fused silica	960
Mirrors	BK-7	1374
Polarizers	BK-7	192
Crystals	KDP/DKDP	576
Windows and Shields	Fused silica	768

The initial laser pulse is generated by the master oscillator and launched into an optical fiber system that amplifies and splits it into 192 separate fibers and transports each pulse to a set of low-voltage optical modulators that shape the pulses in space, time, and frequency, individually for each beam. At this point in the laser chain, the pulse energy is a few nanojoules with duration of several nanoseconds.

These shaped pulses are transported by optical fiber to 48 preamplifier modules (PAM) in the two laser bays. Each PAM contains a ring-resonator regenerative amplifier and a multipass amplifier. The pulse circulates through the ring regenerative amplifier twelve times. The Nd-glass rod in the regenerative amplifier is pumped by semiconductor diode lasers to provide very stable gain and long lifetime without servicing. On exit, the pulse passes through a serrated aperture that converts the round cross-section to a square cross-section, then a four-pass flashlamp-pumped Nd:glass laser boosts the mJ output of the square aperture to a 12.5 J pulse at the TSF. In the PAM, the beams are also smoothed by spectral dispersion to the degree required by either direct or indirect drive targets.

A Galilean telescope placed between the PAM and the "transport" spatial filter (TSF) produces a converging cone of light that enters the main laser beamline by reflection from a small mirror, labeled LM0 in Fig. 2, located near the focal plane

of the TSF. The pulse expands to fill the 40-cm aperture of the spatial filter lens, and is recollimated as it passes through the lens. The pulse then passes next through an amplifier and enters the four-pass laser resonator by reflecting from the dielectric thin-film polarizer. The pulse passes through the Pockels cell optical switch, to which the quarter-wave voltage is applied in order to rotate the plane of polarization of the pulse from vertical to horizontal. The pulse passes next through the "cavity" spatial filter and main amplifier, then reflects from the deformable mirror LM1, which also corrects its wavefront deformation.

By the time the pulse returns to the Pockels cell, the applied voltage has been removed, so the pulse passes through with no change in polarization. The pulse passes through the polarizer and reflects from the second cavity mirror, LM2. The pulse makes a second round trip through the cavity, by which time the Pockels cell voltage has been reapplied to rotate the polarization back to vertical. The pulse then reflects from the polarizer and passes back through the final amplifier and the transport spatial filter on a path slightly displaced from the input path so as to miss the injection mirror LM0.

Beams are transported from the laser bays to the target chamber room in groups of four (2×2 arrays) following the beam paths shown in red in Fig. 2. At the target chamber, the pulses enter the final optics assemblies (FOA), shown in Fig. 3, that convert the 1 μm wavelength to the third harmonic and focus the

pulses onto the fusion target. Each FOA consists of a fused silica vacuum window, potassium dihydrogen phosphate (KDP) frequency conversion crystals, fused silica focus lense, and debris shield that protects the lens from damage by target debris. The debris shield has a diffraction grating etched into its surface to reshape the distribution of laser intensity in the focal spot on the target, and to diffract the residual fundamental and second harmonic wavelength pulses away from the target.

For ignition targets, each beamline must place 95% of its laser energy through a 600 mm spot in the center of the entrance hole of the target. The temporal shape of each pulse has a 15 to 20 ns low-power foot followed by a 3 ns (FWHM) high-power peak; together the 192 beamlines focus as much as 2.2 MJ/600 TW of energy on the target. These figures represent the "redline" of the facility, a 20% design margin over the 1.8 MJ/500 TW requirement for ignition. A wide range of operational modes is available; for example, each beamline can have its own temporal pulse shape.

NIF's integrated computer control system uses a high-speed optical fiber network to connect the approximately 25,000 control points, sensors, and distributed processors in the system. The items that are controlled by computer include motors and switches for alignment, diagnostic systems for the laser

beams, data from target diagnostics, data processing stations, and all other control and information features of the facility.

Principle laser components are described in greater detail in the following paragraphs. A key feature in the design of most of the laser components is that they are composed of modular units that may be quickly replaced while the laser remains in "on-line" status. They are Prototypes of some of these components were built and operated as part of the Beamlet Demonstration Project, described fully in the next section.

1.1 Amplifier

The NIF amplifier module, shown in Fig. 5, is a 4 (high) × 2 (wide) array of neodymium-doped phosphate glass plates, with dimensions of $46 \times 81 \times 4$ cm^3, set vertically on edge at Brewster's angle to the laser beam. Xenon flashlamps, shown in Fig. 6, are mounted vertically to illuminate the four-high stacks of glass slabs, an arrangement resulting in a length that is convenient for the pulsed-power system that drives the flashlamps.

The amplifier modules hang from support frames in order to provide access from the bottom to install and replace laser glass plates, flashlamps, and blast shields. It is extremely important to minimize contamination of the amplifiers by

particles that can burn into the glass surfaces under the intense flashlamp or laser light. Access from the bottom of the amplifiers ensures that service personnel and equipment are always below the sensitive surfaces, so that particles of any debris fall to the floor, not into open amplifier. Amplifier components will be transported and installed by use of a Class 10 clean servicing cart. Fig. 7 illustrates the process of installing a stack of four laser slabs into the amplifier structure using the clean service cart.

The number of amplifier slabs and their distribution, eleven in the main amplifieror a single-pass, small-signal gain of 14.5, and five in the booster, for a single-pass gain of 3.4, were chosen to maximize the output power of the laser over the desired range of pulse shapes. For short pulses, the limit is set by nonlinear effects in the final amplifier. For long pulses, the limit switches over to nonlinear effects in main amplifier and the limit set by the total amount of energy stored in the slabs. Each amplifier unit contains an odd number of slabs to cancel the effects of gain gradients in the end slabs.

1.2 Spatial Filter

Image-relay spatial filters are used in NIF to control growth of intensity noise due to diffraction and self-focusing. The effects of diffraction are reset to zero at the image of the original input profile. The two spatial filters in each NIF beam

image the very uniform intensity profile injected from the preamplifier to a position near the amplifiers and then on to the frequency converter crystals. Nonlinear effects in the laser cause small-scale intensity noise in the laser to grow. This small-scale noise comes to a focus that is displaced to the side of the main focus in the spatial filter, and thus it can be eliminated by placing a small pinhole at the focal plane that blocks this noise while allowing the main beam to go through. Because the intensity near the focal plane is very high, the spatial filters in large lasers such as NIF must be operated in a vacuum to avoid the occurrence of gas breakdown.

1.3 Pockels Cell and Polarizer

A Pockels cell uses electrically induced changes in the refractive index of an electro-optic crystal, such as potassium dihydrogen phosphate (KDP) to rotate the polarization of light. When combined with a polarizer, the Pockels cell serves as an optical switch, directing light into one or the other of two possible paths, depending on the applied voltage.

NIF uses the Plasma Electrode Pockels Cell (PEPC) concept [3] shown in Fig. 8a. In this concept, a thin plate of KDP is placed between two, low pressure helium gas-discharge plasmas. The plasmas serve as electrodes to apply the required longitudinal voltage, but are so tenuous they have no effect on the high-power

laser beam passing through the cell. Fig. 8b shows a prototype plasma electrode Pockels cell with a clear aperture of 35 cm. The device is now operating on Beamlet at the full laser fluence specified for NIF. The polarizer for the switch is a multilayer dielectric coating set at Brewster's angle to the beam.

1.4 Deformable Mirror

The NIF laser must have sufficiently high beam quality to permit focusing the energy from each beam into a half-millimeter diameter circle at the center of the target chamber. While it is possible to purchase optical components finished well enough to achieve this goal, the cost of fabrication is high.

To reduce the tolerances on optics fabrication, NIF will use an adaptive optic system to compensate for distortions in the beam. This system also will compensate for other important distortions, such as thermal gradients. Recent advances in adaptive optics in the Atomic Vapor Laser Isotope Separation program at LLNL, and at several commercial companies and government research facilities, show that the cost of the deformable mirror, sensor, and processor technology required to implement such a system has fallen to the point that adaptive correction systems are very desirable for the NIF facility. Fig. 9 shows a typical deformable mirror that uses electrostrictive actuators to deform the mirror surface to compensate for wavefront errors. This mirror is installed on

Beamlet, and its performance is being studied. NIF will use a similar, but larger, deformable mirror as the cavity mirror LM1 in Fig. 3.

1.5 Frequency Converter

A system of two nonlinear crystal plates of KDP, each approximately $40 \times 40 \times 1$ cm^3, will be used in NIF for frequency conversion to the third harmonic wavelength. The first plate converts two-thirds of the incident 1.05-μm radiation to the second harmonic at 0.53 μm. Then the second crystal mixes that radiation with the remaining 1.05-μm light to produce radiation at 0.35 μm. The conversion process is, of course, power dependent, with required peak efficiency greater than 80%, and overall energy conversion efficiency of 60% for the complex pulse shapes used to drive ignition targets.

A new process to grow crystals of KDP and deuterated KDP at high growth rates is being developed. [4] This process currently is capable of producing crystals , as shown in Fig. 10 with dimensions of 45 cm on the pyramidal faces at growth rates of 15 mm per day. Further development is underway to increase crystal size and optical quality.

1.6 Target Chamber and Diagnostics

The beams enter the target chamber, a 10-m-diameter aluminum sphere, in two conical arrays from the top and two from the bottom through final optics assemblies (FOA), as shown in Fig. 11. The FOA design includes gratings to isolate the 0.35 μm light from residual 1 μm and 0.5 μm illumination. The grating design has been tested in a subscale experiment and proven to be effective in efficiently disposing of the unwanted colors without degrading the desired color. It also allows more flexibility for other pointing and operating frequency configurations.

Twenty-four laser beam ports spaced around the equator of the target chamber permit conversion to direct drive by moving 24 of the indirect-drive final optics assemblies (FOAs) or by later installation of an additional 24 FOAs along with switchable turning mirrors.

Diagnostic instruments, including x-ray spectrometers, microscopes, and cameras, are mounted around the equator and at the poles of the target chamber.

2 BEAMLET DEMONSTRATION PROJECT

Although glass lasers are a relatively mature technology, the NIF laser design is significantly different in many ways from previous lasers. Thus to demonstrate that the NIF system will function as projected, the Beamlet Demonstration Project (henceforth Beamlet) was built. Beamlet was completed in 1994, and is currently operating reliably up through the frequency converters at the full fluence and intensity levels specified for NIF. [5]

To study engineering features of multiple-aperture amplifiers, a 2×2 array was chosen for the Beamlet amplifier. To reduce costs, however, only one of the four apertures in the array contains high-quality laser glass. The other three apertures contain inexpensive glass with absorption properties similar to laser glass. All Beamlet laser components sit on the floor or on optical tables rather than hanging from an overhead support frame as they will on NIF.

Evolution of the NIF design led to other small differences between the Beamlet and the NIF. For example, the beam apertures for the Beamlet are slightly smaller than those for NIF, and the input pulse from the preamplifier is injected into the cavity spatial filter rather than the transport spatial filter. Otherwise, Beamlet has all the NIF components and features shown in Fig. 3.

Fig. 12 is a photograph of the Beamlet facility taken at its completion in 1994. The master oscillator and preamplifier are the same technology as that for NIF, but with only one output channel rather than 192 . The laser pulse reflects from a deformable mirror and enters the cavity transport spatial filter. The deformable mirror was used in this position rather than in the LM1 position described for NIF because this smaller mirror could be adapted from an existing design at very low cost. The pulse then passes through the main amplifier and reflects from mirror LM1, returns through the amplifier and cavity spatial filter to the Pockels cell and LM2, makes a second round trip through amplifier 1, and returns through the Pockels cell to reflect from the polarizer, just as described for NIF.

The output pulse then reflects from three turning mirrors, used to fold the Beamlet optical path to fit the available space. The pulse passes through the final amplifier and the transport spatial filter, then enters the frequency-conversion crystals. Beam splitters direct samples of the infrared and ultraviolet beams to diagnostic instruments located near the frequency converters. Most of the beam energy is absorbed by an absorbing glass beam dump at the end of the beamline.

The Beamlet amplifier, shown in Fig. 13, has a clear aperture is 39 cm, essentially the same as the 40-cm aperture of NIF amplifiers. The amplifiers perform exactly as predicted from design codes validated by experiments on smaller amplifiers.

The large plasma-electrode Pockels cell switch installed on Beamlet is shown in Fig. 8b. Only about 30 J leak through the polarizer when we set this switch to reflect 6 kJ from the polarizer, so the Pockels cell and polarizer are remarkably efficient.

Fig. 14 shows the infrared output energy from Beamlet as a function of the input energy from the preamplifier. For this set of shots, the beam aperture was 34 × 34 cm, a value limited by the 35-cm clear aperture of the Pockels cell crystal. The output energy matches the theoretical model (solid line) very well. The system has delivered up to 13.9 kJ at 5 ns and at somewhat higher output for longer pulses. At 5 ns, the fluence (energy per unit area) across the flat-top part of the beam is 14.3 J/cm^2, 7% above the nominal operating point for NIF.

Initial tests of Beamlet's frequency-conversion crystals, conducted at a beam aperture of 29.6 × 29.6 cm., produced 8.7 J/cm^2 ultraviolet output in 3-ns pulses, 10% above the NIF operating point. The conversion efficiency from infrared to ultraviolet was just over 80% for square pulses, as expected. Frequency conversion tests have also been conducted using the complex shaped pulses required for ignition targets. Conversion efficiency up to 65% was achieved, meeting NIF specifications.

It is important to have very uniform intensity profiles in a fusion laser. Uniform profiles minimize the risk of damage caused by intensity maxima in the beam and help to maintain high frequency-conversion efficiency. Fig. 15 shows intensity profiles of the infrared and ultraviolet beams from Beamlet as recorded by television cameras in the laser diagnostics area. The beam profiles are very smooth and flat across the center, as desired, and they roll off smoothly to zero intensity in a small margin around the edge.

Low phase distortions on the beam are also important. Phase distortions not only prevent the beam from focusing on a small spot, but they also degrade the process of frequency conversion. Fig. 16 shows the distribution of Beamlet energy at the focus of a lens. 95% of the energy is within an angle of ±25 microradians from the center of the spot, well within the NIF requirement of ±35 microradians.

ACKNOWLEDGEMENTS

The work summarized in this review was performed by members of the Inertial Confinement Fusion Program at Lawrence Livermore National Laboratory. A comprehensive account of their individual contributions may be found in the Laser Program Annual Reports for the years 1972-1996, published as internal reports by LLNL, [6] and references cited therein.

REFERENCES

[1] S. W. Haan, S. M. Pollaine, J. D. Lindl, L. J. Suter, R. L. Berger, L. V. Powers, W. E. Alley, P. A. Amendt, J. A. Futterman, W. K. Levedahl, M. D. Rosen, D. P. Rowley, R. A. Sacks, A. I. Shestakov, G. L. Strobel, M. Tabak, S. V. Weber, G. B. Zimmerman, W. J. Krauser, D. C. Wilson, S. V. Coggeshall, D. B. Harris, N. M. Hoffman, and B. H. Wilde, "Design and Modeling of Ignition Targets for the National Ignition Facility", Physics of Plasmas 2 (6), 2480 (1995).

[2] "The National Ignition Facility: An Overview," Energy & Technology Review, UCRL-52000-94-12 (December 1994)

[3] M. A. Rhodes, B. Woods, J. J. DeYoreo, D. Roberts, L.J. Atherton, "Performance of Large-Aperture Optical Switches for High-Energy Inertial-Confinement Fusion Lasers," Appl. Opt. 34 (24), 5312–5325 (1995).

[4] N. P. Zaitseva, J. J. De Yoreo, M. R. Dehaven, R. L. Vital, K. E. Montgomery, M. Richardson and L. J. Atherton, Rapid growth of large-scale (40–55 cm) KH_2PO_4 crystals, J. Cryst. Growth (accepted for publication).

[5] B. M. Van Wonterghem, J. R. Murray, D. R. Speck, and J. H. Campbell, "Performance of the NIF prototype beamlet," Fusion Technol. 26 (3), 702 (1994).

[6] For a comprehensive review, see Laser Program Annual Reports (1972–1996), Lawrence Livermore National Laboratory, Livermore, CA, UCRL-50055-72-96.

FIGURE CAPTIONS

Figure 1. Regions in Power/Energy space where ignition and gain are expected to occur for (a) indirect-drive, and (b) direct-drive targets. In both cases, ignition is predicted to require approximately 1MJ, 400-450 TW drive pulses. Shading indicates margin above ignition achievement. Shaded regions are bounded below by onset of hydrodynamic instabilities and above by laser-plasma interaction instabilities.

Figure 2. Cut-away view of National Ignition Facility and Optics Assembly Buildings.

Figure 3. Single laser beamline of the NIF laser. Path taken by laser pulse is described in the text.

Figure 4. Cut-away view of Final Optics Assembly. Laser beams with 1 μm wavelength enter the packages through the fused silica vacuum window in groups of four , are frequency converted to the third-harmonic wavelength of 0.35 mm, and focused on the target by f/22 fused silica lenses. Diffractive optical element and debris shield is used to control energy distribution on target and prevent damage to optics from target debris.

Figure 5. Cut-away view of NIF amplifier modules. The basic assembly unit is a 4×2 array, one disk deep. Three such units assembled in line are shown in this figure. Each aperture contains a Nd-phosphate glass disk with dimensions of 46 $\times 81 \times 4$ cm^3.

Figure 6. NIF prototype flashlamp is 205 cm long with inside diameter of 4.3 cm. This flashlamp was tested to 39,000 shots without failure.

Figure 7. An ultra-clean maintenance cart that will be used to transport and install amplifier glass slabs and flashlamp cassettes into the overhead support frame.

Figure 8. (a) The Plasma-Electrode Pockels Cell (PEPC) optical switch uses plasma as transparent, high-damage-threshold electrodes to apply longitudinal voltage to the KDP crystal. (b) Prototype large-aperture PEPC installed on Beamlet. This prototype met NIF requirements for timing, efficiency, an stability.

Figure 9. Prototype 7×7 cm^2 deformable mirror currently used on Beamlet. NIF will use the same technology in a 40×40 cm^2 mirror with 39 actuators.

Figure 10. KDP crystal with dimensions for $42 \times 44 \times 37$ cm^3, grown by rapid growth process at 14 mm/day in z direction and 16 mm/day in x-y direction.

Figure 11. Laser beams are transported to the target chamber in groups of four and enter the chamber in two conical arrays from the top and two from the bottom.

Figure 12. Photograph of Beamlet Facility.

Figure 13. Beamlet 2 × 2 amplifier module. Each beamline has clear aperture of 39×39 cm^2.

Figure 14. Performance of Beamlet for 34×34 cm^2 beam at three pulse lengths. Solid line is prediction of theoretical model of amplifier performance.

Figure 15. Spatial intensity profiles for Beamlet fundamental wavelength (a) and third harmonic (b).

Figure 16. Focal spot distribution of Beamlet pulse energy. Approximately 95% of the energy is within +/– 25 microradians of the center of the spot, well within NIF requirement.

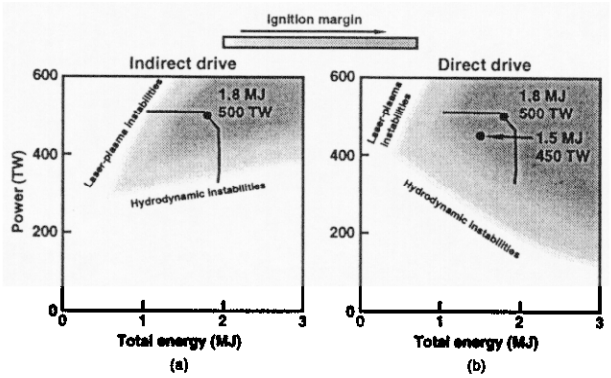

Direct drive has more potential upside (bigger accessible ignition region with NIF), but more uncertainty

W. H. Lowdermilk
Inertial Confinement Fusion Program at Lawrence Livermore National Laboratory: the National Ignition Facility, Inertial Fusion Energy, 100–1000 TW Lasers, and the Fast Ignitor Concept

50-00-0498-0704Apb02
3SWHlmcm

Figure 1 (a) & (b)

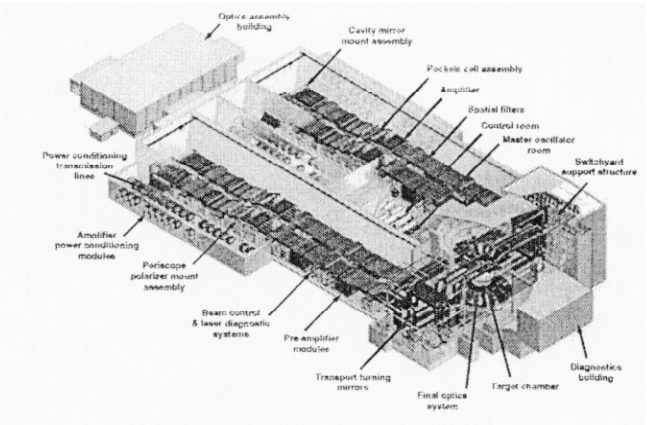

W. H. Lowdermilk
Inertial Confinement Fusion Program at Lawrence Livermore National Laboratory: the National Ignition Facility, Inertial Fusion Energy, 100–1000 TW Lasers, and the Fast Ignitor Concept

40-00-0998-2100Apb01
03GAD/dougherty

Figure 2

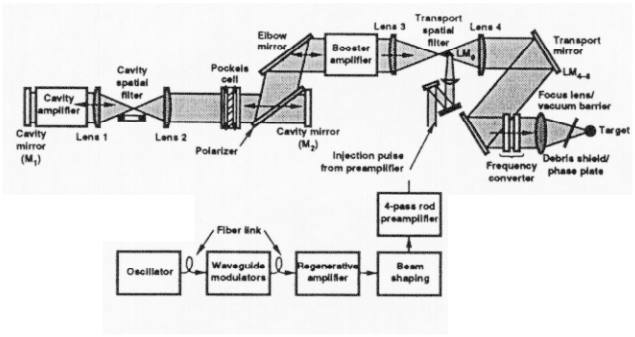

W. H. Lowdermilk
Inertial Confinement Fusion Program at Lawrence Livermore National Laboratory: the National Ignition Facility, Inertial Fusion Energy, 100–1000 TW Lasers, and the Fast Ignitor Concept

40-00-0394-0789pb08

Figure 3

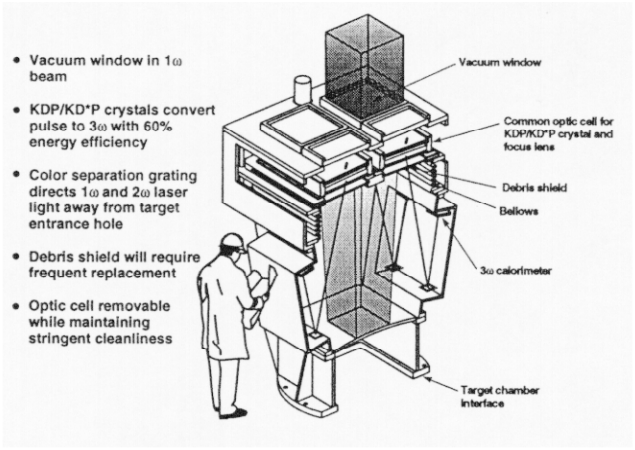

W. H. Lowdermilk
Inertial Confinement Fusion Program at Lawrence Livermore National Laboratory: the National Ignition Facility, Inertial Fusion Energy, 100–1000 TW Lasers, and the Fast Ignitor Concept

40-00-0294-0800pb02
26JAPsmo

Figure 4

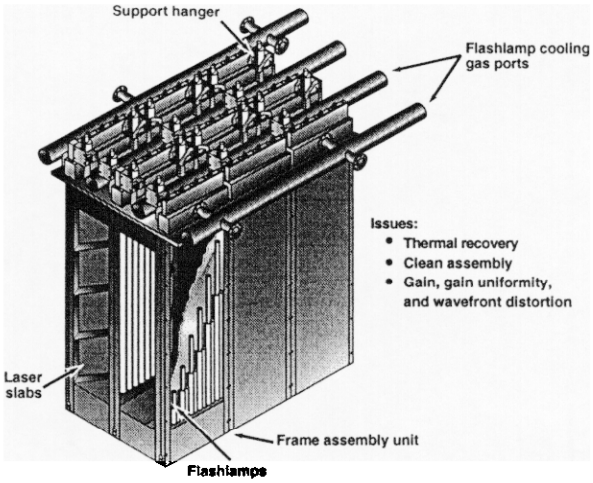

W. H. Lowdermilk
Inertial Confinement Fusion Program at Lawrence Livermore National Laboratory: the National Ignition Facility, Inertial Fusion Energy, 100–1000 TW Lasers, and the Fast Ignitor Concept

70-50-0696-2174Bpb02
2JTH/sae

Figure 5

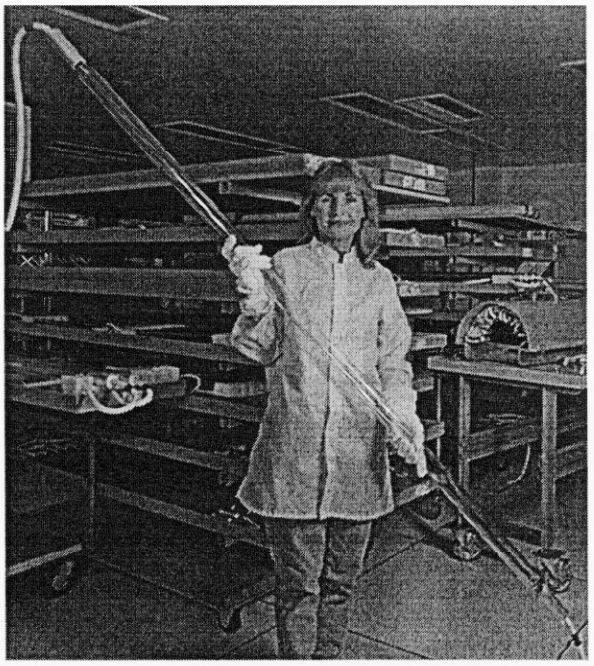

W. H. Lowdermilk
Inertial Confinement Fusion Program at Lawrence Livermore National Laboratory: the National Ignition Facility, Inertial Fusion Energy, 100–1000 TW Lasers, and the Fast Ignitor Concept

70-00-0796-1807Bpb02
24LEZ/sae

Figure 6

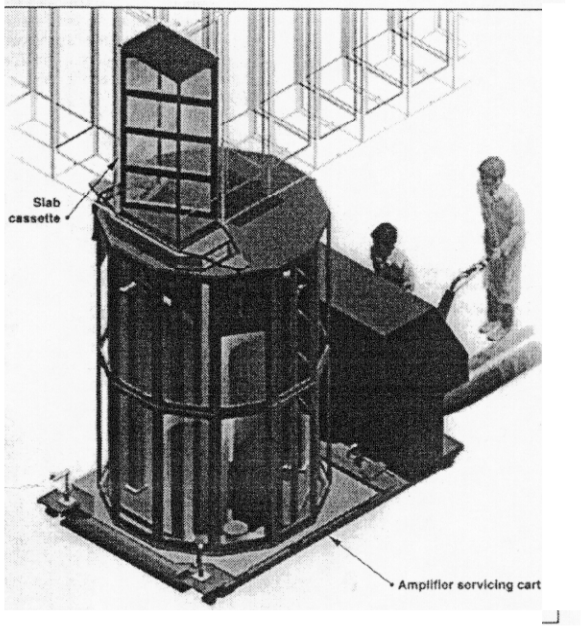

W. H. Lowdermilk
Inertial Confinement Fusion Program at Lawrence Livermore National Laboratory: the National Ignition Facility, Inertial Fusion Energy, 100–1000 TW Lasers, and the Fast Ignitor Concept

03WJH/gbh

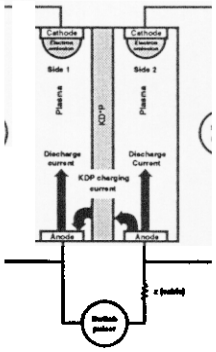

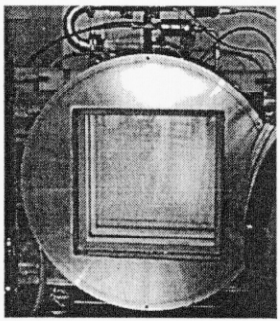

W. H. Lowdermilk
Inertial Confinement Fusion Program at Lawrence Livermore National Laboratory: the National Ignition Facility, Inertial Fusion Energy, 100–1000 TW Lasers, and the Fast Ignitor Concept

70-60-0492-1254Fpb01
27JAP/lw

Figure 8

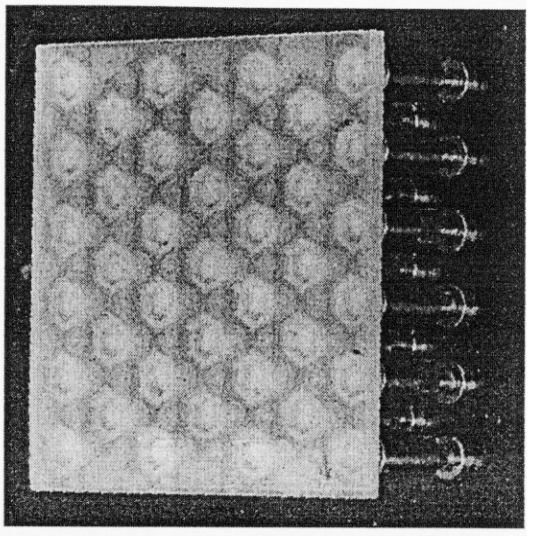

W. H. Lowdermilk
Inertial Confinement Fusion Program at Lawrence Livermore National Laboratory: the National Ignition Facility, Inertial Fusion Energy, 100–1000 TW Lasers, and the Fast Ignitor Concept

Figure 8

- **Crystal dimensions 42 x 44 x 37 cm can yield several NIF PEPC crystals**
- **Grown in 27 days**
  - **14 mm/day in z direction**
  - **16 mm/day in x-y plane**

W. H. Lowdermilk
Inertial Confinement Fusion Program at Lawrence Livermore National Laboratory: the National Ignition Facility, Inertial Fusion Energy, 100–1000 TW Lasers, and the Fast Ignitor Concept

40-00-0796-1662Spb01
1594ARvaa

Figure 10

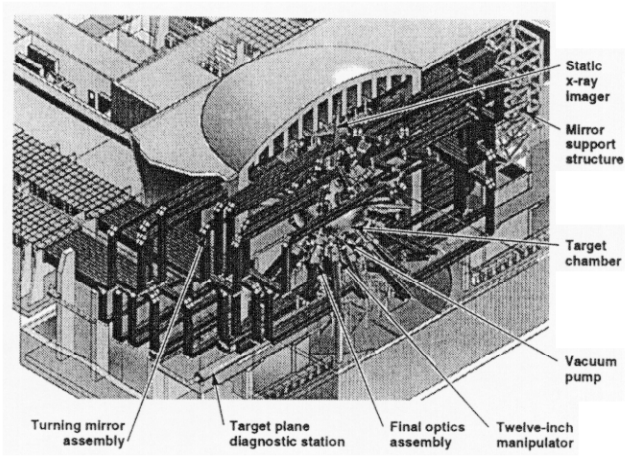

W. H. Lowdermilk
Inertial Confinement Fusion Program at Lawrence Livermore National Laboratory: the National Ignition Facility, Inertial Fusion Energy, 100–1000 TW Lasers, and the Fast Ignitor Concept

40-00-0694-2685pb02

03WJHgbh

Figure 11

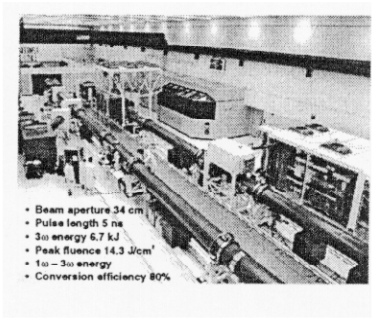

W. H. Lowdermilk
Inertial Confinement Fusion Program at Lawrence Livermore National Laboratory: the National Ignition Facility, Inertial Fusion Energy, 100–1000 TW Lasers, and the Fast Ignitor Concept

70-50-0494-1561pb01

15MAR/sas

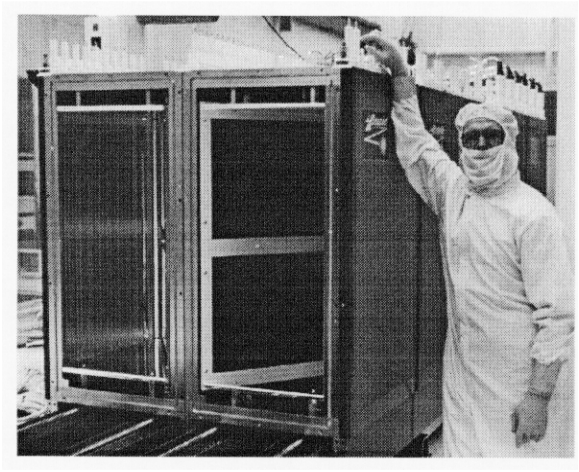

W. H. Lowdermilk
Inertial Confinement Fusion Program at Lawrence Livermore National Laboratory: the National Ignition Facility, Inertial Fusion Energy, 100–1000 TW Lasers, and the Fast Ignitor Concept

70-50-1098-3500pb01
/ms

Figure 13

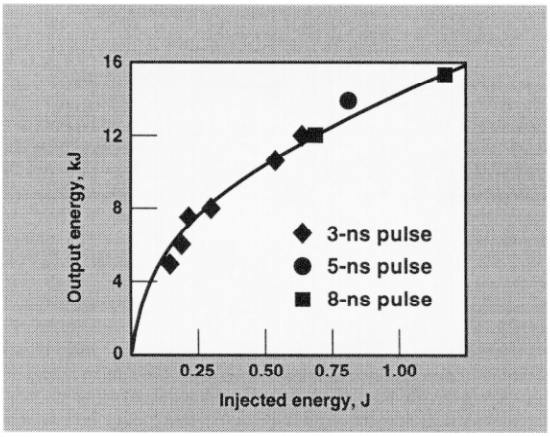

W. H. Lowdermilk
Performance of the Beamlet amplifier for a 34- x 34-cm beam at three different pulse lengths. The infrared output energy is plotted as a function of the input or injected energy from the preamplifier. This plot shows that the output energy matches our theoretical model (solid line) quite well.

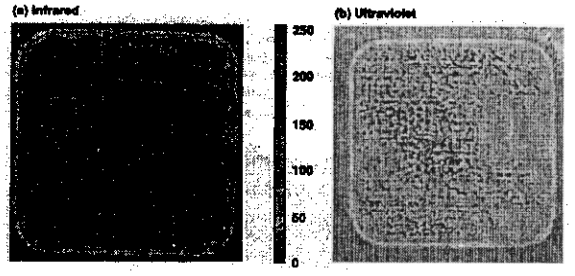

W. H. Lowdermilk
Inertial Confinement Fusion Program at Lawrence Livermore National Laboratory: the National Ignition Facility, Inertial Fusion Energy, 100–1000 TW Lasers, and the Fast Ignitor Concept

[illegible]

Figure 15

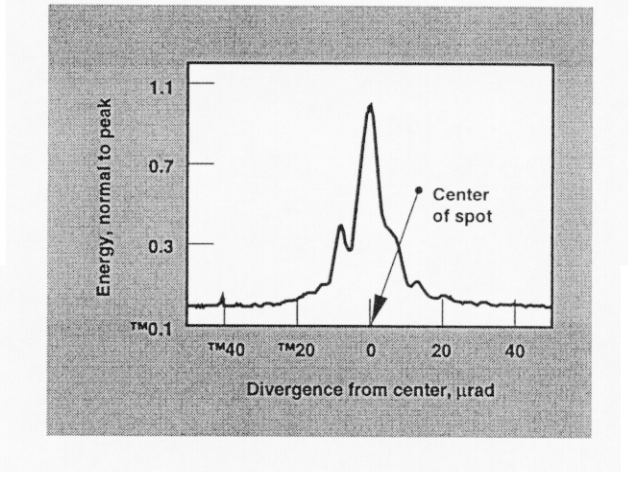

W. H. Lowdermilk
Inertial Confinement Fusion Program at Lawrence Livermore National Laboratory: the National Ignition Facility, Inertial Fusion Energy, 100–1000 TW Lasers, and the Fast Ignitor Concept

Figure 16

Technical Information Department • **Lawrence Livermore National Laboratory**
University of California • Livermore, California 94551